

Effect of building proximity on external and internal pressures under tornado-like flow

G.R. Sabareesh¹, Shuyang Cao^{*2}, Jin Wang², Masahiro Matsui³ and Yukio Tamura⁴

¹*BITS Pilani Hyderabad Campus, Hyderabad, India*

²*State Key Lab of Disaster Reduction in Civil Engineering, Tongji University, Shanghai, China*

³*Tokyo Polytechnic University, Atsugi, Kanagawa, Japan*

⁴*Chongqing University, China, and Tokyo Polytechnic University, Japan*

(Received October 17, 2017, Revised December 22, 2017, Accepted January 18, 2018)

Abstract. Tornadoes are one of the world's deadliest natural phenomena. They are characterized by short life span and danger. It has been observed through post-damage surveys that localities with large numbers of buildings suffer major damage during a tornado attack resulting in huge loss of life and property. Thus, it is important to study interfering buildings exposed to tornado-like vortices. The present study focuses on external and internal pressures developed on building models exposed to translating tornado-like vortices in the presence of an interfering building model. The effects of translating speed and swirl ratio of a tornado-like vortex on external and internal pressures for a principal building in the vicinity of an interfering building are investigated. Results indicate that external and internal pressures are enhanced or reduced depending on the location of the interfering building with respect to the principal building.

Keywords: tornado-like flow; interference effects; external pressures; internal pressures; translating speed

1. Introduction

Past studies including post-damage surveys have reported on the effect of tornadoes on civil engineering structures. Many post-damage surveys give an account of the extent of damage inflicted on buildings and classify the tornado under the Fujita scale (Pinelli and O'Neill 2000). But to understand better the interaction between tornadoes and structures, laboratory scaled simulators are developed that are capable of imitating real-world tornadoes. Properly scaled building models exposed to these vortex interactions give an insight into pressure coefficients on both the external and internal surfaces of the building.

Many past researchers, such as Mehta *et al.* (1976) and McDonald and Marshall (1982), have performed post-damage surveys to evaluate damage inflicted by a tornado. These surveys have provided information about the extent of damage and probable wind speeds were estimated from it. Attempts to numerically simulate a tornado-like vortex to understand its effects on building models are also reported.

Dutta *et al.* (2002) investigated the dynamic responses of structures to tornado loads using Finite Element Methods. They found that not only lateral wind speeds but also translational speeds of tornadoes are important as they may influence the effects of resonance. Selvam and Millet, 2003 performed computer modeling of tornado forces on buildings. Governing equations used were non-linear and boundary conditions used bring limitations to these studies.

Past researchers also tried to simulate vortices in laboratory scale simulators. A detailed account of some of these earlier works using stationary tornado-like flow simulators are reported in Mishra *et al.* (2008a, b), Sabareesh *et al.* (2012, 2013a, b). More recently, translating type tornado simulators have been used to estimate wind loads considering both the rotational and translating natures of tornado-like vortices. Haan *et al.* (2010) studied aerodynamic loads on single story buildings exposed to tornado-like vortices using a translating tornado-like-flow simulator at Iowa State University. Since then translating tornado-like-flow simulators of different sizes have been developed in Tokyo Polytechnic University and Tongji University to enable more realistic study on tornado effects on structures.

Many past studies have reported on the effects of tornado-like flows on single isolated structures. Chang (1971) investigated a cubic model kept at predefined locations with respect to a stationary vortex and found that the pressure distributions on the cube face showed combined effects of suction and dynamic pressures. Jischke and Light (1983) obtained force and moment coefficients for a rectangular structure exposed to a tornado vortex. They found that addition of swirl to flow can affect the forces and moments experienced by rectangular structures when compared to that under boundary layer flow. Mishra *et al.* (2008a, b) characterized the flow field under a stationary tornado-like-flow simulator and compared the pressure coefficients of a cubic model exposed to tornado-like flow with those of a cube exposed to boundary-layer flow. They found that a building model exposed to tornado-like flow and boundary-layer flow may experience completely different and opposite forces. Sabareesh *et al.* (2012, 2013a, b), investigated the effect of swirl ratio,

*Corresponding author, Professor
E-mail: shuyang@tongji.edu.cn

building location and ground roughness on building models exposed to a stationary tornado-like flow. The authors found that the mean and peak pressure coefficients vary significantly with respect to building location, swirl ratio and ground roughness. Cao *et al.* (2015) investigated wind pressures experienced by a cooling tower exposed to a tornado-like vortex. Results indicate the combined effects of pressure drop accompanying a tornado and aerodynamic flow structure interaction on the surface pressures experienced by the cooling tower. In most of these studies a single principle building or structure was considered and the effects of surrounding buildings in the path of the tornado was not taken into account. Also, many of these studies failed to consider the translating effects of tornado vortices.

Zhang and Sarkar (2009) performed experiments on tornado-induced wind loads and flow patterns on a group of low-rise gable-roof buildings and investigated the effects of spacing and height ratio of surrounding buildings to test buildings and building orientations. The authors found that there was a reduction in horizontal load resulting from the sheltering effect of surrounding buildings. Zhang and Sarkar (2010) investigated the flow around a two-story gable-roof building surrounded by a group of buildings using Particle Image Velocimetry (PIV). They found that a complicated vortex system was induced by tornado-like wind. The effect of swirl ratio and translating speeds on the wind loads were not discussed by the authors. Refan *et al.* (2014) attempted to establish a relationship between laboratory parameters of simulated tornado-like vortices and the Enhanced Fujita Scale. The authors concluded that the WindEEE Dome facility could generate tornado-like vortices similar to EF0- to low-end EF3-rated tornadoes. Refan and Hangan (2016) characterized the tornado-like flow fields in the model scale wind testing chamber WindEEE Dome using flow visualization, surface pressure tests and PIV measurements. The authors found that a range of tornado-like vortices ranging from a single cell to two cells could be generated in this facility. The facility also enabled the decoupling of effects of swirl ratio from that of radial Reynolds number. Tang *et al.* (2017) conducted experiments on a large-scale tornado simulator, VorTECH, to study the effects of aspect ratio on tornado-like vortices. The authors reported that the mean characteristics of flow and surface pressure deficit depend critically on swirl ratio and aspect ratio. Sabareesh *et al.* (2016) compared the pressure coefficients experienced by an isolated building to those experienced by a building in the presence of an interfering building for a single translating speed. The authors found that the presence of an interfering building can either enhance or reduce the surface pressures on building faces exposed to tornado-like flow depending on the location of the interfering model.

Most previous studies only considered the surface pressures on isolated building models and many failed to consider the effects of translating speeds and swirl ratio. It is reported in the literature that the translating speed of a full-scale tornado can vary from 10-20 m/s (Refan *et al.* 2014), which then combines with the dynamic effects such as swirl ratio and may produce complex wind environments. Under these situations, buildings in the

proximity may experience varying wind loads. The present investigation focuses on external and internal pressures experienced under tornado-like flow by a building model in the presence of an interfering building. The interfering building model was placed at different locations with respect to the principal building both in tandem as well as in oblique directions. The effect of translating speeds and swirl ratio of the generated tornado-like flow on the external and internal pressure coefficients were investigated to enable a better understanding of the wind loads in a more realistic environment in the presence of another building in close proximity.

2. Damage survey

A post-damage survey of a tornado that occurred in the city of Noshiro, Akita Prefecture, Japan in 2009, (Matsui *et al.* (2009), provided the motivation for this study. The damage survey revealed that many buildings in the tornado's path were destroyed either partially or completely, and dominant openings were created in them. It was also observed that buildings with neighboring buildings in their vicinity suffered varying degrees of damage, as can be seen from the footprints of damage in Fig. 1. This demonstrates the need to understand the effect of nearby buildings on the external and internal pressures developed on the building under consideration.

3. Experimental setup

The experimental setup used in the present study is essentially the same as that used by Cao *et al.* (2015) at Tongji University, as shown in Fig. 2. The characteristic dimensions of the simulator includes an updraft of 0.5 m diameter, in which the height of the inflow layer can be varied. For the present set of experiments the inflow layer height was fixed at 300 mm above the floor to maintain a regulated inflow to the simulator center to achieve control over the flow's dynamic characteristics. Guide vanes at the top of the simulator provided the required swirl to the flow. By adjusting their orientation, different swirl ratios could be obtained. The swirl ratio in the present case is defined as $S = \tan \phi / 2 a$, where ' ϕ ' corresponds to the guide vane angle and a is the aspect ratio defined as H/r_o , where ' H ' is the inflow height and r_o is the updraft hole radius. In the present study, the guide vanes were adjusted to keep the inflow height and updraft hole radius the same to obtain two swirl ratios $Sw1=0.36$ and $Sw2=0.72$.

The simulator could translate at a maximum speed of 0.4 m/s over the simulator floor, on which the interfering and building model were located. Four different translating speeds of the simulator's updraft system were considered : 0.06 m/s, 0.12 m/s, 0.18 m/s and 0.24 m/s. Typical full scale translational speeds of tornadoes are of the order of 10- 20 m/s (Refan *et al.* 2014). Thus, the translating speeds used in the simulator will scale to the order of 1:170-1:85.

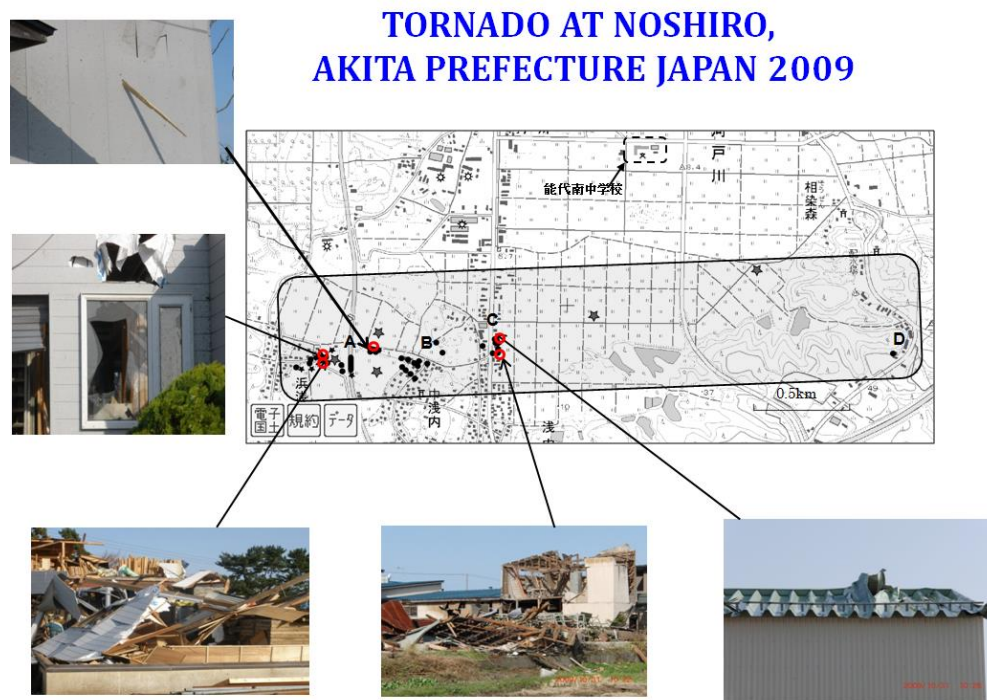


Fig. 1 Footprints of tornado damage



Fig. 2 Experimental Setup-Tornado Like flow Simulator at Tongji University

Two identical cubical building models were used: one as a principal building and other as an interfering building.

The principal building model was located at the center of the simulator floor. The interfering building was placed at five locations with respect to the principal building. These locations were in line with the building centerline (tandem locations) and at oblique angles to the principal building, see Figs. 3(a) and 3(b). The locations were non-dimensionalized with respect to the characteristic building dimension. The locations of the principal building model and the interfering model, the radius of the tornado vortex generated, and layout of pressure taps on principal building model are shown in Figs. 4(a) and 4(b).

4. Velocity measurements

In the absence of the building models, the velocity components were measured above the simulator floor at a height equal to that of the building model height. A TFI Cobra probe with a four-hole head 2.6 mm in diameter and a frequency response of 0 Hz to 2 kHz was used for the measurement. This probe is capable of measuring wind speeds from 2 m/s to 100 m/s within a cone of influence of $\pm 45^\circ$. Velocity measurement using the Cobra probe can be considered reasonably accurate outside the tornado vortex core, but of low accuracy for velocities less than 2m/s in the tornado center. The sampling frequency for this

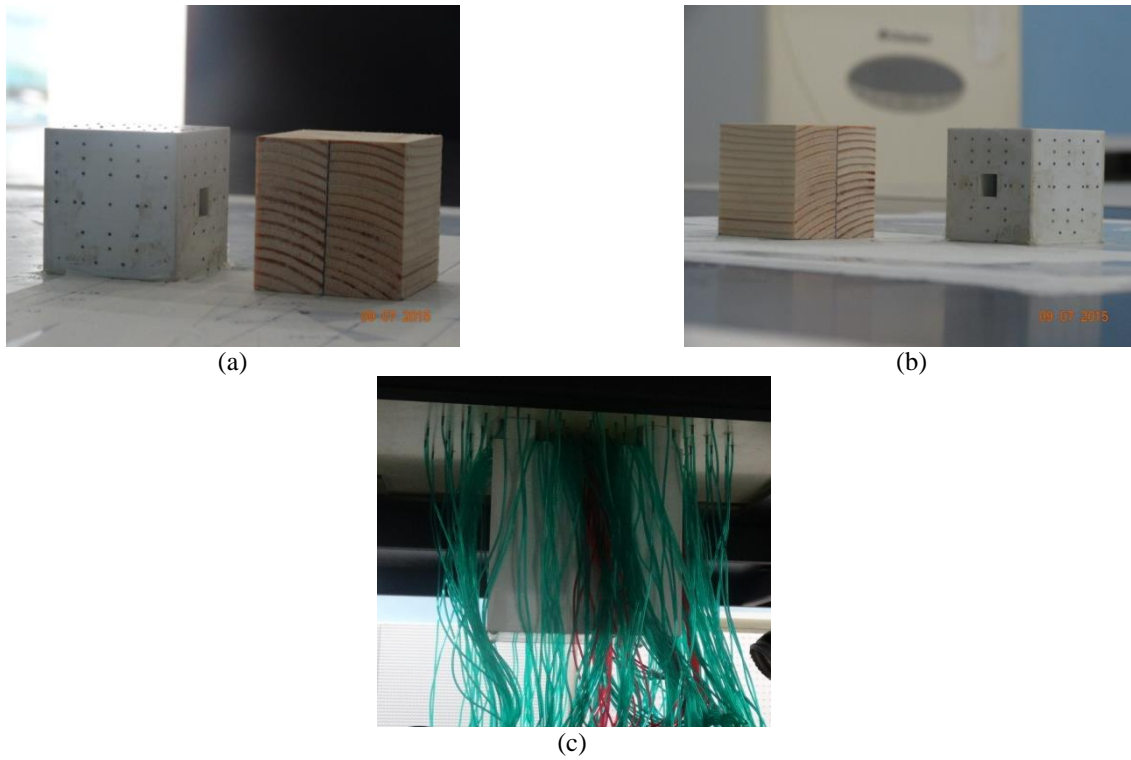


Fig. 3 Principal Building and Interfering Building Models-(a) Tandem locations, (b) Oblique Locations and (c) Volume chamber beneath simulator floor

present set of experiments was 700 Hz, see Cao *et al.* (2015). The tornado simulator was translated at the same speed across the simulator floor for multiple runs and the average maximum tangential velocity under each translating speed measured at simulator center corresponding to building roof height was used to calculate the dynamic pressure, which was in turn used for normalizing to obtain pressure coefficients (Haan *et al.* 2010, Cao *et al.* 2015).

To determine tornado vortex radius, a stationary vortex was positioned at the simulator center. Velocity components were measured using the Cobra probe at different radial locations across the vortex, keeping the measurement height the same as the building height. The tornado vortex radius was determined as 110 mm at the radius of maximum winds, see Fig. 5.

5. Pressure measurement

The principal and interfering building models considered in this study were cubic models each of side 50mm. The principal building was made of acrylic and instrumented with pressure taps and had a dominant opening in one of its four walls with an opening porosity of 4%. A total of 102 pressure taps were distributed over its external surfaces on its roof and side walls, see Figs. 4(b) and 4(b) were distributed on its internal surfaces. The pressure taps were in turn connected using nylon tubes to multi-channel high-speed pressure scanners. The pressures recorded on the external and internal surfaces were sampled at 300Hz and converted to pressure coefficients. The

reference static pressure (P_∞) was measured far from the vortex, which represents the atmospheric pressure, as in previous studies (Haan *et al.* 2010, Sabareesh *et al.* 2012).

As discussed in the previous section, the reference dynamic pressure (q_r) was calculated using the maximum velocity (V) at roof height in the absence of the model. The external and internal surface pressures were captured as the tornado translated from one end of the simulator to the other. The pressure coefficient is given by Eqs. (1) and (2).

$$Cp_j = \frac{P_j - P_\infty}{q_r} \quad (1)$$

$$q_r = \frac{1}{2} \rho V^2 \quad (2)$$

The minimum pressure coefficients ($Cpe (min)$ and $Cpi(min)$) in the time history of pressures were taken for analysis. These represent the largest pressures experienced by the building in the entire translational path of tornado. In the present investigation, internal volume scaling was performed to account for the distortion of internal volume that may take place in model scale, as given by Eq. (3). λ_{vol} , λ_L and λ_v are volumetric, length and velocity scales, respectively.

$$\lambda_{vol} = \lambda_L^3 / \lambda_v^2 \quad (3)$$

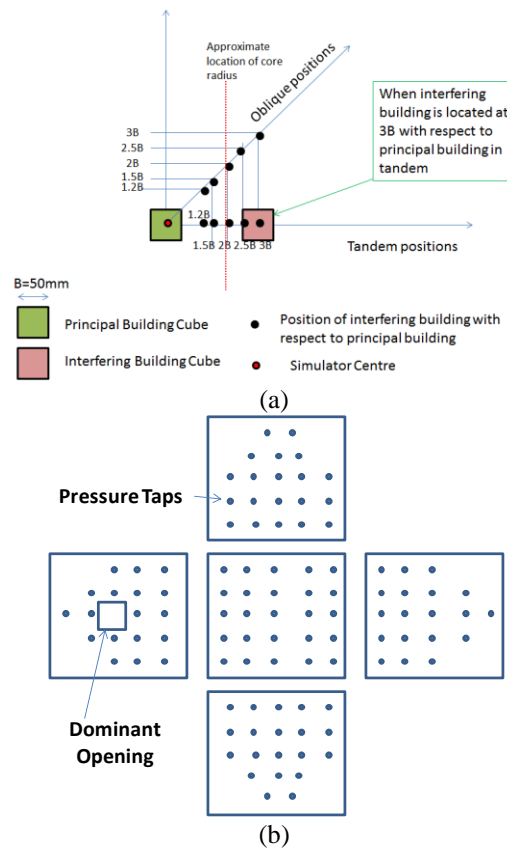


Fig. 4 (a) Different positions of interfering building model with respect to principal building and (b) Layout of pressure taps on exploded view of building model

This also maintain similarity in the dynamic response between full scale and model scale (Trygvasson 1979, Holmes 1979, Oh *et al.* 2007, Sabareesh *et al.* 2013). Thus, a scaled volume chamber was placed beneath the simulator floor to achieve this volume scaling, see Fig. 3(c).

Assuming a uniform pressure distribution inside the building model and the volume chamber, the average internal pressure coefficients were obtained and plotted for different interfering building locations.

6. Results and discussion

The principal building model was stationed at the center of the simulator and the interfering model was placed at different locations. The positions identified were 1.2B, 1.5B, 2B, 2.5B and 3B in both tandem and oblique configurations as shown in Fig. 4(a), where 'B' is the side dimension of the principal building model. Different side walls were identified as Windward (W), Right Wall (S1), Left Wall (S2), Leeward (L) and Roof (R) observed in the direction of tornado translation. Pressure coefficients were obtained as described earlier and the worst cases of pressure coefficients experienced by each wall were compared for different swirl ratios and also for different translating speeds. The following sections describe the effect of these parameters on the external and internal surface pressure coefficients.

6.1 Effect of translating speed

The laboratory scale tornado-like flow generated was allowed to translate at different speeds and the effects of translating speed on both external and internal pressure coefficients of the principal building for different positions of interfering building were investigated. The worst case pressure coefficients experienced by each wall and roof of principal building model at each location and configuration were taken for comparison.

It can be seen in Fig. 6 that for a translating speed of 0.06m/s and oblique arrangement of interfering building, the roof and windward wall experienced the largest pressure coefficients at location 1.2B. As the interfering building model was shifted to location 1.5B, the windward wall experienced higher magnitudes than the roof, which was reversed for locations greater than 1.5B. Side wall S2 continued to experience the lowest pressure coefficient for all locations of interfering building model. The pressure coefficients experienced by the different walls were in the range -0.8 to -1.2 as can be seen in the Fig. 6.

Comparing this with the interfering building positions in tandem directions for the same translating speeds, see Fig. 7, it can be seen that the behaviors of the pressure coefficients on the roof and windward wall were almost opposite to those experienced when the interfering building was in an oblique direction. The roof experienced the largest pressure coefficients at location 1.2B, which became nearly equal to

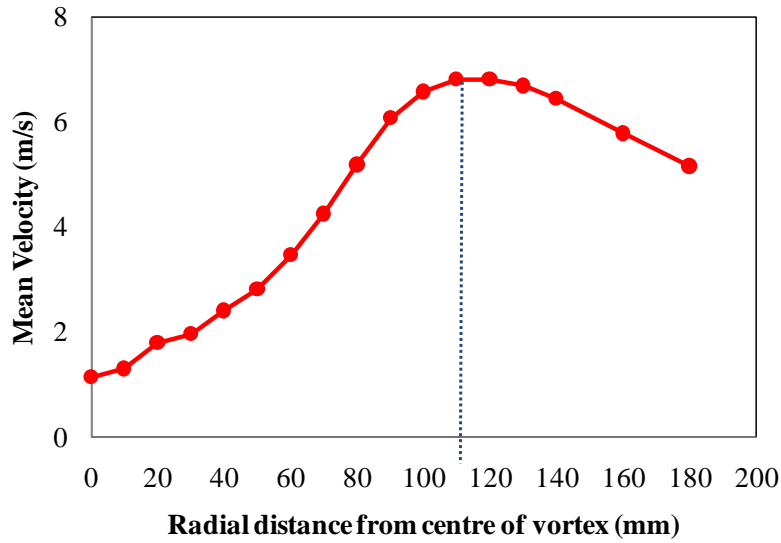


Fig. 5 Variation of velocity from the center of vortex and location of core radius (Sabareesh *et al.*2016)

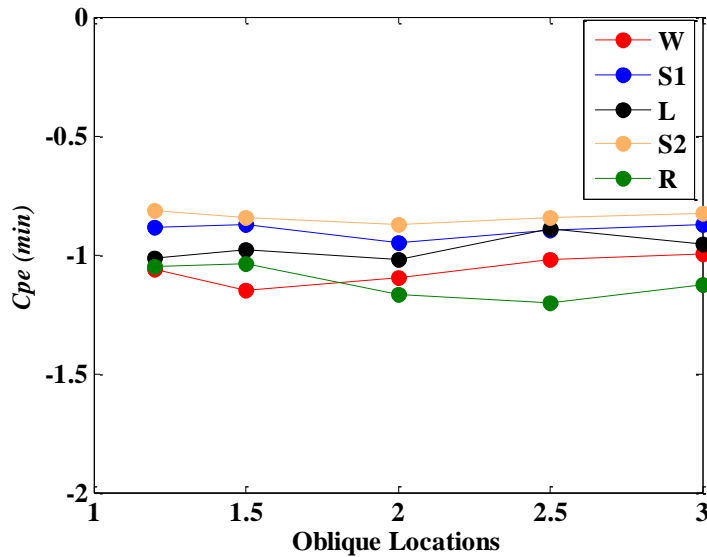


Fig. 6 Minimum external pressure coefficients on building walls and roof- translating speed 0.06m/s, for oblique interfering building model locations

that of the windward wall at location 1.5B, which further decreased at locations 2B and 2.5B and became nearly equal to that of the windward wall at the farthest location 3B. For tandem locations, side walls S1 and S2 showed comparable pressure coefficients, as the translating flow was nearly symmetrical to both these side walls. The internal pressure coefficients, as can be seen in Figure 8, showed comparable values $Cp = -0.7 \sim -0.8$ irrespective of configuration and location. Thus, the windward wall under tandem locations was experiencing a sheltering effect as evident from the lower pressure coefficients. But the effect on the internal pressures was negligible for all locations.

As can be observed from Fig. 9, for a translating speed of 0.12 m/sec and oblique arrangement, the trend in variation of pressure coefficients on windward wall and roof with respect to the position of the interfering building model were similar to that for a translating speed of 0.06m/s, but the magnitudes of variation were significant, $Cp = -2.5 \sim -2.75$, compared to the lower translating speed case. It is to be noted that the dynamic pressure used to calculate the pressure coefficient in each case was obtained from the maximum velocity of the tornado flow, averaged over multiple runs, at model roof height for the respective translation speed. At locations 2B and 3B, the leeward and windward walls were experiencing comparable pressure

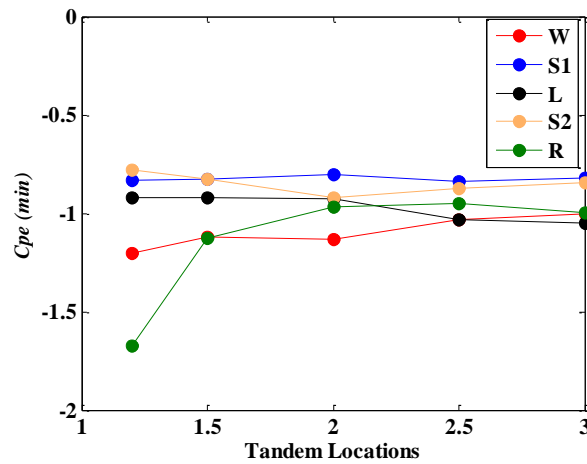


Fig. 7 Minimum external pressure coefficients on building walls and roof- translating speed 0.06 m/s, for tandem interfering building model locations

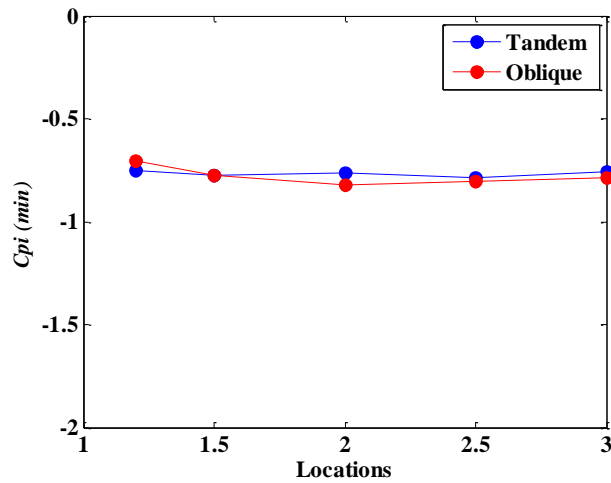


Fig. 8 Minimum internal pressure coefficients for translating speed 0.06 m/s, for different building model locations

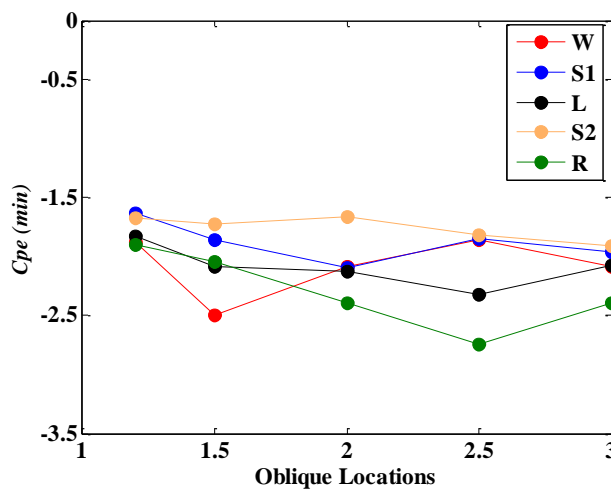


Fig. 9 Minimum external pressure coefficients on building walls and roof- translating speed 0.12 m/s, for oblique interfering building model locations

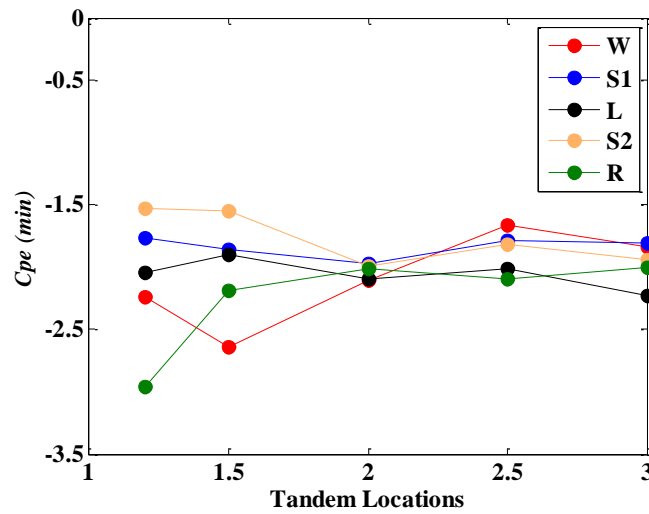


Fig. 10 Minimum external pressure coefficients on building walls and roof- translating speed 0.12 m/s, for tandem interfering building model locations

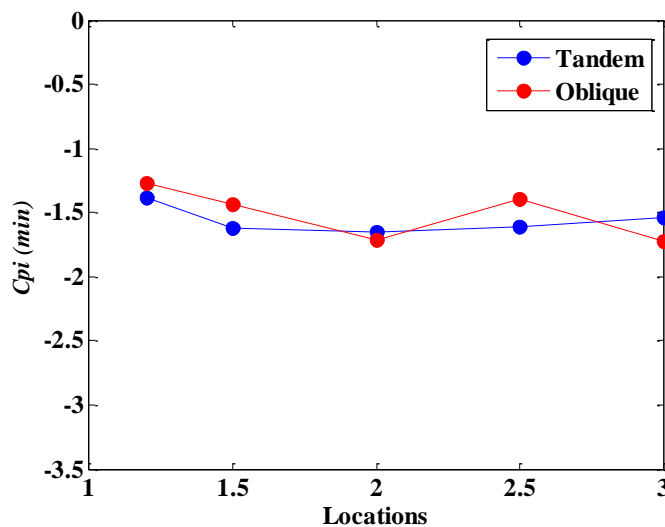


Fig. 11 Minimum internal pressure coefficients for translating speed 0.12 m/s, for different building model locations

coefficients to those observed for 0.06m/s. Thus, the shielding effect from the interfering building was least felt at these locations. The variations among different walls were minimum at location 1.2B of interfering building, which increased as the location was shifted through 1.5B, 2B and 2.5B and gradually decreased for location 3B. This can be attributed to the relative angle at which the incident tornado-like flow impinges on the different walls.

Analyzing the tandem arrangement of interfering building model for a translating speed of 0.12m/sec, it can be seen from Fig.10 that the variations among pressure coefficients on different walls were appreciable ($C_p = -1.5 \sim -3$) at 1.2B location, and ($C_p = -1.5 \sim -2.6$) at 1.5B location, which may be attributed to the diminishing wind loads on those walls which are obstructed by the upstream

interfering building. Also, it was observed that the pressure coefficients decreased to a minimum at location 2B. Locations 2.5B and 3B registered variations among pressure coefficients on different walls, but they were not as significant as those of locations 1.2B or 1.5B. At location 1.2B, similar to the case of translating speed of 0.06m/s, the roof experienced a larger pressure coefficient ($C_p = -3$) than the windward wall ($C_p = -2.23$), whereas for both these translating speeds, at oblique location 1.2B, the pressure coefficients on the windward wall and roof were comparable, which is an interesting observation, as can be seen in Figs. 6 and 9. This may be because the windward wall at these locations was completely shielded from the incident translating tornado-like flow by the interfering building, whereas the suction pressure experienced by the

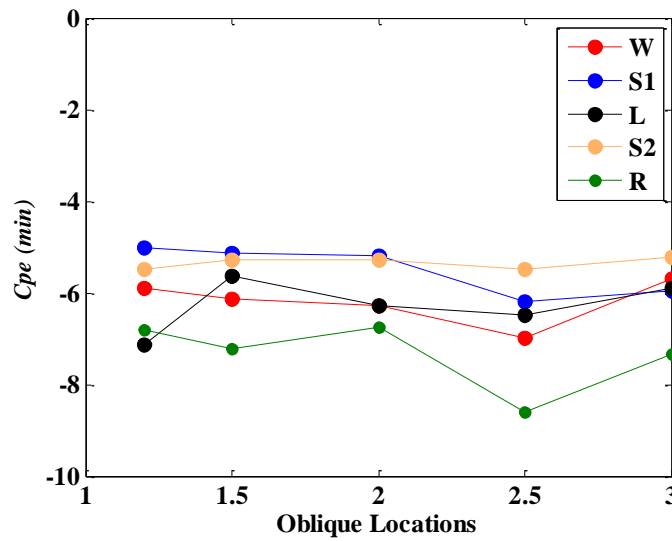


Fig. 12 Minimum external pressure coefficients on building walls and roof-translating speed 0.18 m/s, for oblique interfering building model locations

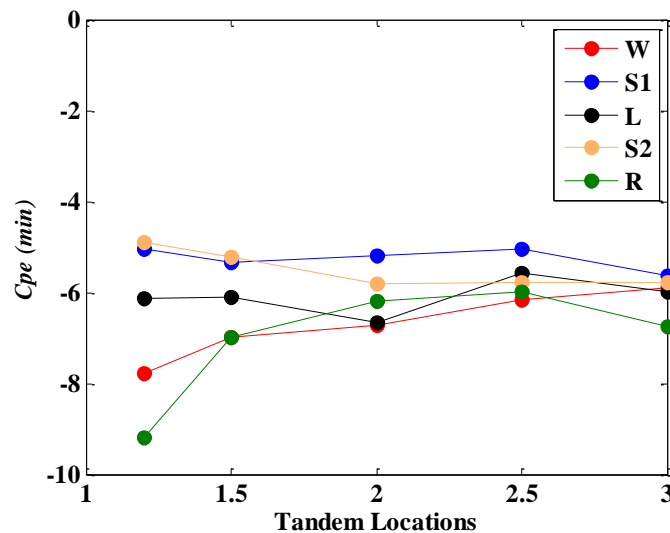


Fig. 13 Minimum external pressure coefficients on building walls and roof- translating speed 0.18 m/s, for tandem interfering building model locations

roof will remain high as the vortex center traverses over it. Another notable observation was that for these two translating speeds of 0.06m/s and 0.12 m/s, the interfering model at tandem location 1.2B resulted in a wide variation of pressure coefficients on different walls of principal building model, whereas the corresponding location of interfering building in oblique configuration resulted in minimum variation among walls. The internal pressure coefficients experienced by the principal building model under tandem configuration experienced slightly larger pressure coefficients irrespective of location than those for oblique configuration, as can be seen in Fig. 11. This may be because the building under tandem location will be in the

trajectory of the translating tornado, and thus may be completely engulfed within the central low pressure region of the tornado vortex as it translates over it.

For a translating speed of 0.18m/sec, it can be observed in Fig. 12, that for oblique locations of interfering building model, the roof continued to experience the largest pressure coefficients ($C_p=-7.2$), compared to other walls in all locations. Side wall S2 experienced comparable pressure coefficients ($C_p=-5.2$) at all locations of interfering model, whereas side wall S1 showed larger pressure coefficients at locations 2.5B and 3B compared to those at earlier locations.

When observing the pressure coefficients for tandem locations of interfering model for translating speed 0.18

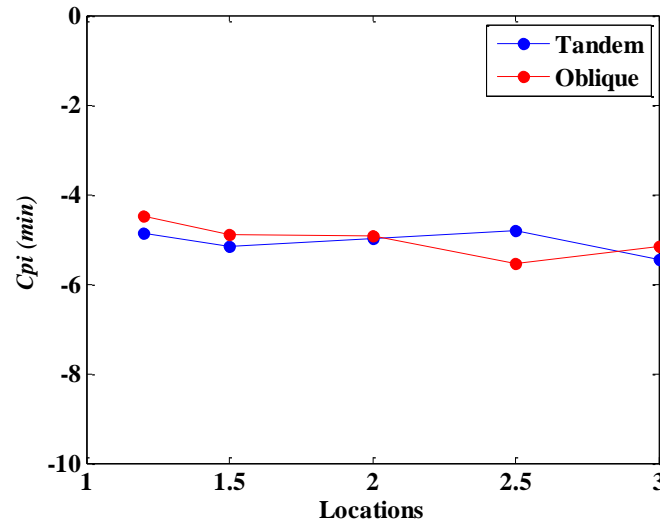


Fig. 14 Minimum internal pressure coefficients for translating speed 0.18 m/s, for different building model locations

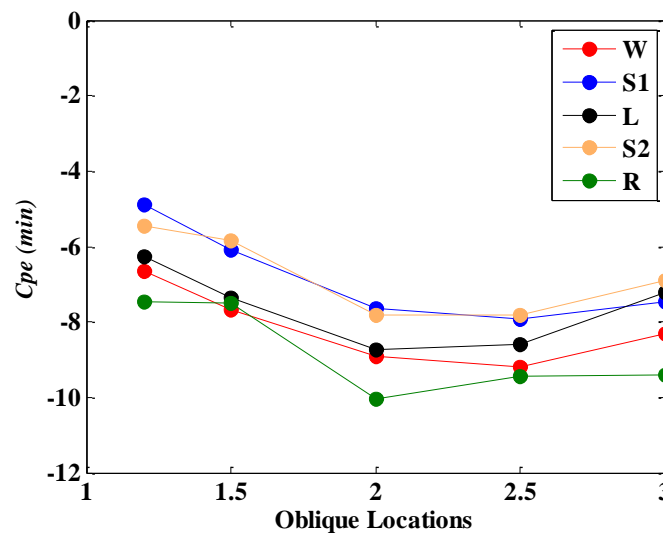


Fig. 15 Minimum external pressure coefficients on building walls and roof- translating speed 0.24 m/s, for oblique interfering building model locations

m/sec, see Fig. 13, it was observed that the variation between walls ($C_p = -4.9 \sim -9.17$) was predominant at location 1.2B and progressively decreased as the location of interfering model was advanced from that of the principal building model. The roof experienced larger pressure coefficients at location 1.2B, whereas at location 1.5B, the roof as well as the windward wall experienced comparable values of pressure coefficient. For locations 1.2B, 1.5B, and 3B, side walls S1 and S2 experienced comparable pressure coefficients, but at locations 2B and 2.5B, side wall S1 registered smaller pressure coefficients. The pressure coefficients experienced by building model walls, specifically windward as well as roof, in tandem locations 1.2B and 1.5B, ($C_p = -7.8$ and $C_p = -9.17$ respectively) were considerably larger than those in corresponding oblique

locations ($C_p = -5.9$ and $C_p = -6.8$ respectively). The internal pressure coefficients experienced by the principal building model for the two configurations, tandem and oblique, for translating speed 0.18 m/sec are shown in Fig. 14. Although the pressure coefficients were larger than those of lower translating speed cases, the trend of variation at different locations was similar.

Analyzing the nature and magnitude of pressure coefficients for a translating speed of 0.24 m/s and an oblique configuration, see Fig. 15, the pressure coefficients on different walls of principal building showed a steady increase in magnitude as the interfering building model was advanced from 1.2B to 2B. For 0.18m/sec translating speed for oblique locations, the roof continued to experience the largest pressure coefficients ($C_p = -10.05$ at 2B), compared

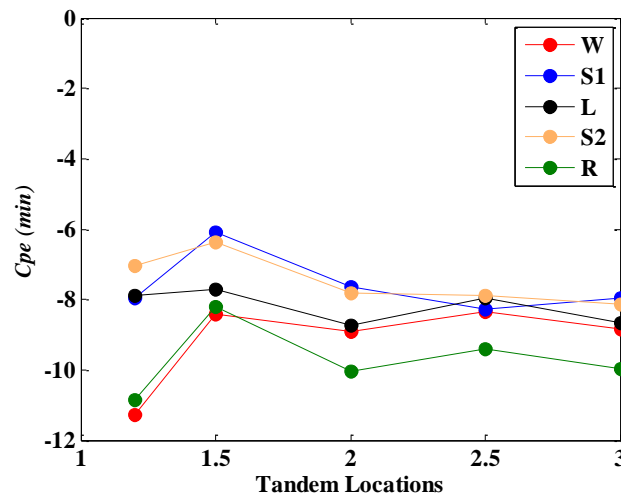


Fig. 16 Minimum external pressure coefficients on building walls and roof- translating speed 0.24 m/s, for tandem interfering building model locations

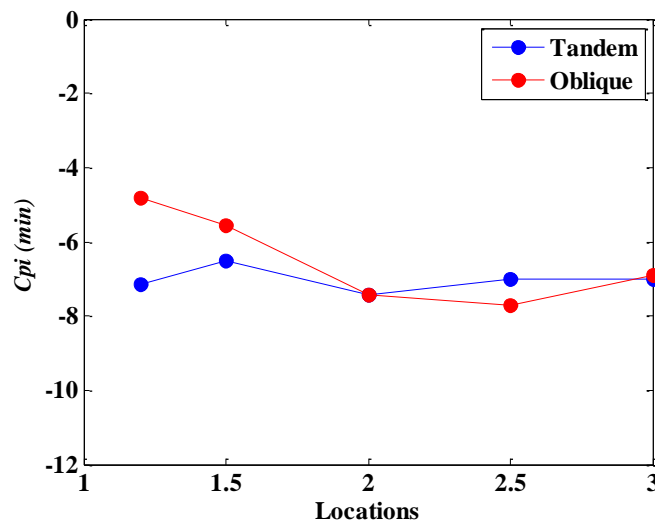


Fig. 17 Minimum internal pressure coefficients for translating speed 0.24 m/s, for different building model locations

to all walls at all locations analyzed. The side walls experienced comparable magnitudes of pressure coefficients except for the nearest and farthest location of interfering model to the principal building model.

For the different tandem locations analyzed, see Fig. 16, it was observed that at location 1.2B, the variation was maximum between pressure coefficients of different walls ($C_p = -7.0 \sim -11.3$). The windward wall experienced larger pressure coefficients for locations 1.2B and 1.5B than the roof, and reversed for locations greater than 1.5B. The side walls experienced comparable pressure coefficients for all locations. The internal pressure coefficients showed considerable variation for locations 1.2B and 1.5B for the two configurations tandem and oblique, as observed in Fig. 17, but at later locations the variations in internal pressure coefficients were minimum.

In almost all cases analyzed, the leeward wall experienced a pressure coefficient between those on the side walls on the one hand and on the roof and windward walls on the other. This was observed for both tandem and oblique locations.

Thus, tornado translation speed, location of interfering building with respect to translating flow and translation direction with respect to building walls determines the magnitude and nature of pressure coefficients on different walls.

6.2 Effect of Swirl ratio

Tornado-like flow was generated for two swirl ratios $Sw1=0.36$ and $Sw2=0.72$. Pressure coefficients were compared for a single translating speed of 0.12 m/s and building locations 1.2B, 1.5B and 2B. The dynamic

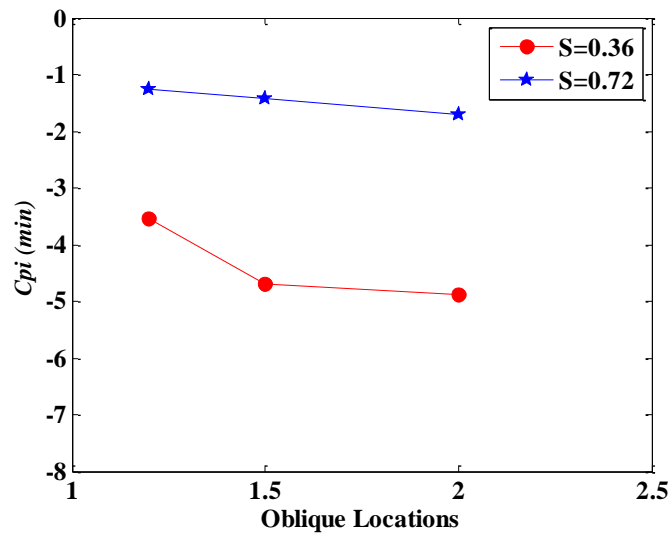


Fig. 18 Minimum internal pressure coefficients for different swirl ratios-Oblique Locations

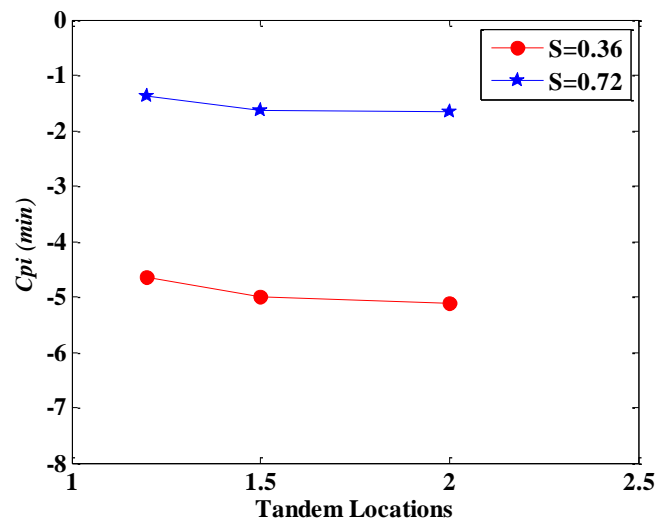


Fig. 19 Minimum internal pressure coefficients for different swirl ratios-Tandem Locations

pressure in each case was obtained by using the maximum velocity, averaged over multiple runs, corresponding to the respective swirl ratio as described in the previous section.

It is observed from Figs. 18 and 19 that irrespective of swirl ratio and configuration in which the interfering building is placed, as the interfering building was moved farther from the principal building model, the internal pressure coefficient showed an increasing trend.

It can be observed from Figs. 20 and 21 that for the windward wall, W, as the interfering building model was moved in either tandem or oblique direction, for Swirl ratio $Sw2=0.72$, the pressure coefficients gradually increased first as it was moved from 1.2 to 1.5 and then decreased as the location of the interfering building was shifted to 2B. However, for swirl ratio $Sw1=0.36$, it was observed that the pressure coefficients decreased as the interfering model was

moved away from the principal building model in either tandem or oblique directions. This decrease was more drastic for tandem locations than for oblique locations. Thus, a lower swirl effect was found to increase wind loads on the windward wall of the principal building at 1.2B more than for other locations.

For the leeward wall, L, it can be seen that, for Swirl Ratio $Sw2=0.72$, the location of interfering building did not have any significant effect on the magnitude of external pressure coefficients. However, for $Sw1=0.36$, it was observed that as the interfering model was moved in the tandem direction, the pressure coefficients increased further, whereas for oblique locations, the pressure coefficients slightly decreased.

For side walls to the translating flow, irrespective of swirl ratio, for tandem locations of building model, the

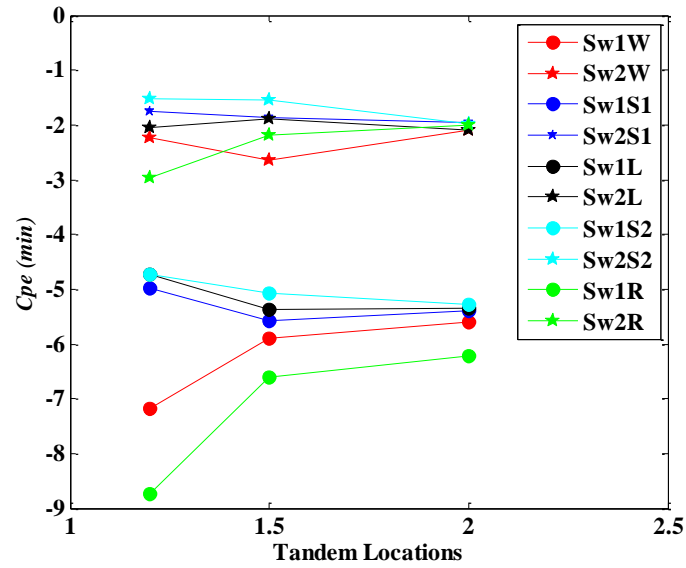


Fig. 20 Comparison of minimum external pressure coefficients on different building walls for different swirl ratios ($Sw1=0.36$ & $Sw2=0.72$)-Tandem Locations

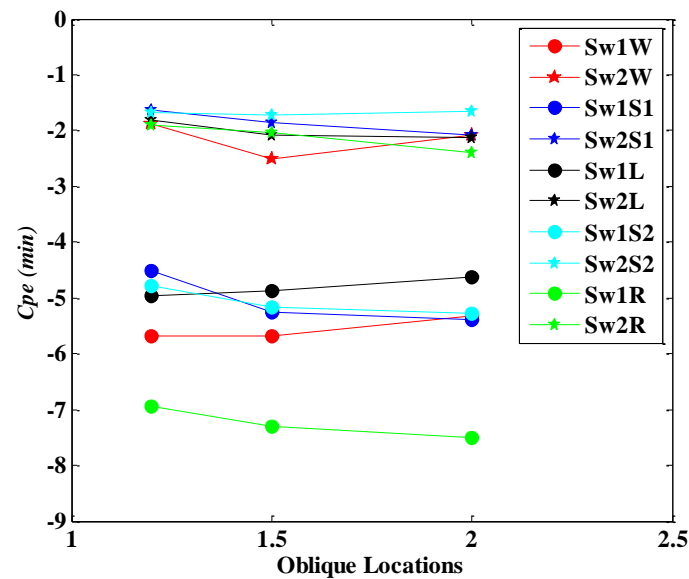


Fig. 21 Comparison of minimum external pressure coefficients on different building walls for different swirl ratios ($Sw1=0.36$ & $Sw2=0.72$)-Oblique Location

decrease in pressure coefficients for side wall S1 were comparable with that of side wall S2, whereas for the oblique direction, the side wall S2 showed similar pressure coefficients for all locations of interfering building model for $Sw2=0.72$. However, the pressure coefficients increased for side wall S1. For swirl ratio $Sw1=0.36$, for side wall S2, the pressure coefficient increased as the interfering building was moved away from the principal building, whereas for side wall S1, the increase was more significant. This may be because the side wall may be located perpendicular to the tangential flow of the tornado vortex at this location.

Comparing the worst case of pressure coefficients experienced by the roof, R, it can be observed that for oblique locations, for both $Sw1=0.36$ and $Sw2=0.72$, the pressure coefficients increased, whereas the trend reversed as the interfering model was moved in the tandem direction. There was a significant decrease in pressure coefficient between tandem locations 1.2B and 1.5B; the building under the lower swirl flow registered an appreciable decrease compared to the one under higher swirl.

7. Conclusions

Interfering building models were analyzed to determine the effects of translating speed and swirl ratio of a laboratory tornado-like flow on external and internal pressure coefficients. Some noteworthy observations include

- (1) The roof face experienced the largest pressure coefficients for tandem locations. This may be because the roof face gets completely engulfed within the central low pressure region of the tornado vortex as it translates over it. This higher suction on roofs may be a reason for roof uplifts seen in many post-tornado-damage investigations.
- (2) At oblique locations, windward walls and roof faces experienced the largest pressure coefficients at locations 1.2B, but at tandem locations, the interfering building provided a sheltering effect, reducing wind induced pressures on the windward wall.
- (3) For most analyzed translating speeds, there were considerable differences among the pressure coefficients experienced by different walls when the interfering building model was at locations 1.2B and 1.5B, tandem locations, whereas the oblique locations did not produce a similar variation in pressure coefficient for the corresponding locations irrespective of translating speeds. This may be due to the sheltering effect produced by the building model upstream under tandem location on the tornado-wind-induced pressures.
- (4) Side walls of the building model to translating flow experienced lower pressure coefficients than windward and leeward walls and roof.
- (5) The internal pressure coefficients under each translating speed showed a trend similar to those of the pressure coefficients experienced by the side walls and were comparable in both tandem and oblique locations.
- (6) Internal pressure coefficients increased with increase in distance of interfering building with respect to principal building for the two swirl ratio cases analyzed. This may be because at farther locations, as the tornado translates over the building, a strong updraft flow along with a high tangential velocity component may result in a higher negative pressure on the building interior in the presence of a dominant opening in the form of a window or one created by flying debris.
- (7) The trend of external pressure coefficient variation on the roof was similar for both swirl ratios analyzed, but the windward wall showed considerable variations, which may be attributed to the differences in magnitude of tangential velocity flow components impinging the windward face under the two swirl flow regimes.
- (8) Lower pressure coefficients were experienced for higher swirl ratio case $S=0.72$ compared to $S=0.36$, when the reference dynamics pressure in each case was obtained at the building model roof height in the absence of the model.

The present investigation thus gives a better understanding of the effects of translating speed and swirl ratio on the external and internal pressures experienced by a building model in the presence of an interfering building at different locations and possible reasons for the damage to roofs and walls observed through post tornado damage

survey.

Acknowledgements

The authors wish to acknowledge the financial support from the National Natural Science Foundation of China (NSFC) Grant No. 51720105005, the Cooperative Research Program of Civil Engineering College of Tongji University No. TMGFXX-2015-003 and Fundamental Research Funds for the Central Universities No. 22120170255 towards the experiments at Tongji University, Shanghai. The authors would also like to acknowledge the support received from the TPU-JURC Program and BITS-Pilani, Hyderabad Campus.

References

- Cao S., Wang, J., Cao J., Zhao, L. and Chen, X., (2015), "Experimental study of wind pressures acting on a cooling tower exposed to stationary tornado-like vortices", *J. Wind Eng. Ind. Aerod.*, **145**, 75-86.
- Chang, C.C. (1971), "Tornado wind effects on buildings and structures with laboratory simulation", *Proceedings of the 3rd International Conference on Wind Effects on Buildings and Structures*, 231-240.
- Dutta, P.K., Ghosh, A.K. and Agarwal, B.L. (2002), "Dynamic response of structures subjected to tornado loads by FEM", *J. Wind Eng. Ind. Aerod.*, **90**, 55-69.
- Haan, F.L. Jr., Balaramudu, V.K. and Sarkar, P.P. (2010), "Tornado-induced wind loads on a low rise building", *J. Struct. Eng.*, **136**(1), 106-116.
- Holmes, J.D. (1978), Mean and fluctuating internal pressures induced by wind. Department of Civil and Systems Engineering, James Cook University of North Queensland, 435-450.
- Jischke, M.C. and Light, B.D. (1983), "Laboratory simulation of tornadic wind loads on a rectangular model structure", *J. Wind Eng. Ind. Aerod.*, **13**, 371-382.
- Matsui, M., Tamura, Y., Cao, S., Yoshida, A., Kobayashi, F., Okada, R. and Sabareesh, G.R. (2009), Recent tornado damage in Japan, International Forum on Tornado Disaster Risk Reduction, Dhaka, Bangladesh.
- McDonald, J.R. and Marshall, T.P. (1983), Damage survey of the tornadoes near Atlas, Oklahoma on May 11, 1982. Available from Wind Science and Engineering Research Center, Texas Tech University.
- Mehta, K.C., Minor, J.E. and McDonald, J.R. (1976), "Wind speed analysis of April 3-4 tornadoes", *J. Struct. Div.-ASCE*, **102**(9), 1709-1724.
- Mishra, A.R., James, D.L. and Letchford, C.W. (2008a), "Physical simulation of a single-celled tornado-like vortex, Part A: Flow field characterization", *J. Wind Eng. Ind. Aerod.*, **96**, 1243-1257.
- Mishra, A.R., James, D.L. and Letchford, C.W. (2008b), "Physical simulation of a single-celled tornado-like vortex, Part B: Wind loading on a cubic model", *J. Wind Eng. Ind. Aerod.*, **96**, 1258-1273.
- Oh, J.H., Kopp, G.A. and Incelet, D.R. (2007), "The UWO contribution to the NIST aerodynamic database for wind loads on low buildings: Part 3. Internal pressures", *J. Wind Eng. Ind. Aerod.*, **95**, 755-779.
- Pinelli, J.P. and O'Neill, S. (2000), "Effect of tornadoes on residential masonry structures", *Wind Struct.*, **3**(1), 23-40.
- Refan, M. and Hangan, H. (2016), "Characterization of tornado-like flow fields in a new model scale wind testing chamber", *J.*

- Wind Eng. Ind. Aerod.*, **151**, 107-121.
- Refan, M., Hangan, H. and Wurman, J. (2014), "Reproducing Tornadoes in laboratory using proper scaling", *J. Wind Eng. Ind. Aerod.*, **135**, 136-148.
- Sabareesh, G.R., Cao, S., Wang, J., Matsui, M. and Tamura, Y. (2016), "Studies on interference effects of building models exposed to tornado-like vortex", *Proceedings of the 8th International Colloquium on Bluff Body Aerodynamics and Applications*, Boston.
- Sabareesh, G.R., Matsui, M. and Tamura, Y. (2012), "Dependence of surface pressures on a cubic building in tornado like flow on building location and ground roughness", *J. Wind Eng. Ind. Aerod.*, **103**, 50-59.
- Sabareesh, G.R., Matsui, M. and Tamura, Y. (2013a), "Characteristics of internal pressure and resulting roof wind force in tornado-like flow", *J. Wind Eng. Ind. Aerod.*, **112**, 52-57.
- Sabareesh, G.R., Matsui, M. and Tamura, Y. (2013b), "Characteristics of tornado vortex developed under a translating tornado-like flow simulator", *Proceedings of the 8th Asia Pacific Conference on Wind Engineering*, Chennai, India.
- Selvam, R.P. and Millet, P.C. (2003), "Computer modeling of tornado forces on buildings", *Wind Struct.*, **6**(3), 209-220.
- Tang, Z., Wu, L., Feng, C., Zuo, D. and James, D. (2017), "Effects of aspect ratio on tornado-like vortices simulated in a large-scale tornado-simulator", *Proceedings of the 13th Americas Conference on Wind Engineering*, Florida, U.S.A.
- Tryggvason, B.V. (1979), "Aero elastic modeling of pneumatic and tensioned fabric structures", *Proceedings of the 5th International Conference on Wind Engineering*, Colorado State University.
- Ward, N.B. (1972), "Exploration of certain features of tornado dynamics using a laboratory model", *J. Atmos. Sci.*, **29**, 1194-1204.
- Zhang, W. and Sarkar, P.P. (2009), "Influence of surrounding buildings on tornado-induced wind loads of a low-rise building", *Proceedings of the 11th Americas Conference on Wind Engineering*, San Juan, Puerto Rico.
- Zhang, W. and Sarkar, P.P. (2010), "Influence of surrounding buildings on the flow around a low-rise building in ABL and tornado-like winds", *Proceedings of the 5th International Symposium on Computational Wind Engineering (CWE2010)*, North Carolina, USA.

